Tuberous sclerosis complex and Myc coordinate the growth and division of *Drosophila* intestinal stem cells

Alla Amcheslavsky,[1] Naoto Ito,[1] Jin Jiang,[4,5] and Y. Tony Ip[1,2,3]

[1]Program in Molecular Medicine, [2]Program in Cell Dynamics, and [3]Department of Cell Biology, University of Massachusetts Medical School, Worcester, MA 01605
[4]Department of Developmental Biology and [5]Department of Pharmacology, University of Texas Southwestern Medical Center, Dallas, TX 75390

Intestinal stem cells (ISCs) in the adult *Drosophila melanogaster* midgut can respond to damage and support repair. We demonstrate in this paper that the tuberous sclerosis complex (TSC) plays a critical role in balancing ISC growth and division. Previous studies have shown that imaginal disc cells that are mutant for *TSC* have increased rates of growth and division. However, we report in this paper that loss of TSC in the adult *Drosophila* midgut results in the formation of much larger ISCs that have halted cell division. These mutant ISCs expressed proper stem cell markers, did not differentiate, and had defects in multiple steps of the cell cycle. Slowing the growth by feeding rapamycin or reducing Myc was sufficient to rescue the division defect. The *TSC* mutant guts had a thinner epithelial structure than wild-type tissues, and the mutant flies were more susceptible to tissue damage. Therefore, we have uncovered a context-dependent phenotype of *TSC* mutants in adult ISCs, such that the excessive growth leads to inhibition of division.

Introduction

Stem cell–mediated repair is a promising approach for treating a variety of pathological disorders. Many adult tissues contain stem cells, and tissue homeostasis requires replenishment of lost cells by these adult stem cells. An imbalance between the removal of dead cells and the production of new cells can lead to tissue overgrowth, tissue damage, inflammation, and cancer (Niemeyer et al., 2006; Nystul and Spradling, 2006; Metcalfe and Ferguson, 2008).

In the adult mammalian intestine, stem cells are located near the base of each crypt (Crosnier et al., 2006; Yen and Wright, 2006; Walker and Stappenbeck, 2008; Barker et al., 2009). Two groups of cells, called label retention cells and columnar base cells, have stem cell properties but express completely different markers (Barker et al., 2007; Montgomery and Breault, 2008; Sangiorgi and Capecchi, 2008; Zhu et al., 2009; Li and Clevers, 2010). These intestinal stem cells (ISCs) give rise to progenitor cells in the transit-amplifying zone and provide a large number of precursor cells that can replenish cells of various lineages along the crypt-villus axis. However, the mechanism by which these different ISCs and progenitor cells mediate intestinal repair remains to be investigated (Barker et al., 2008; Batlle, 2008; Scoville et al., 2008; Casali and Batlle, 2009).

In the adult *Drosophila melanogaster* midgut, ISCs are present individually and distributed evenly underneath the epithelium (Micchelli and Perrimon, 2006; Ohlstein and Spradling, 2006). When an ISC divides, it gives rise to a renewed stem cell and an enteroblast (Fig. 1 A). Immediately after division, a higher level of active cytoplasmic Delta is retained in the cell that remains as an ISC, whereas the neighboring enteroblast quickly loses the active form of Delta (Bray, 2006; Ohlstein and Spradling, 2007). This asymmetric level of active Delta in ISCs stimulates the Notch signaling pathway in the newly formed enteroblast (Bardin et al., 2010), which ceases division and starts to differentiate. Depending on the strength of Notch pathway stimulation, the enteroblast may differentiate to become an enterocyte or enteroendocrine cell (Micchelli and Perrimon, 2006; Ohlstein and Spradling, 2006, 2007).

Correspondence to Tony Ip: Tony.Ip@umassmed.edu

Abbreviations used in this paper: dsRNA, double-stranded RNA; DSS, dextran sulfate sodium; EdU, 5-ethynyl-2′-deoxyuridine; InR, insulin receptor; ISC, intestinal stem cell; MARCM, mosaic analysis with repressible cell marker; TOR, target of rapamycin; TSC, tuberous sclerosis complex; UAS, upstream activation sequence.

The Rockefeller University Press $30.00
J. Cell Biol. Vol. 193 No. 4 695–710
www.jcb.org/cgi/doi/10.1083/jcb.201103018

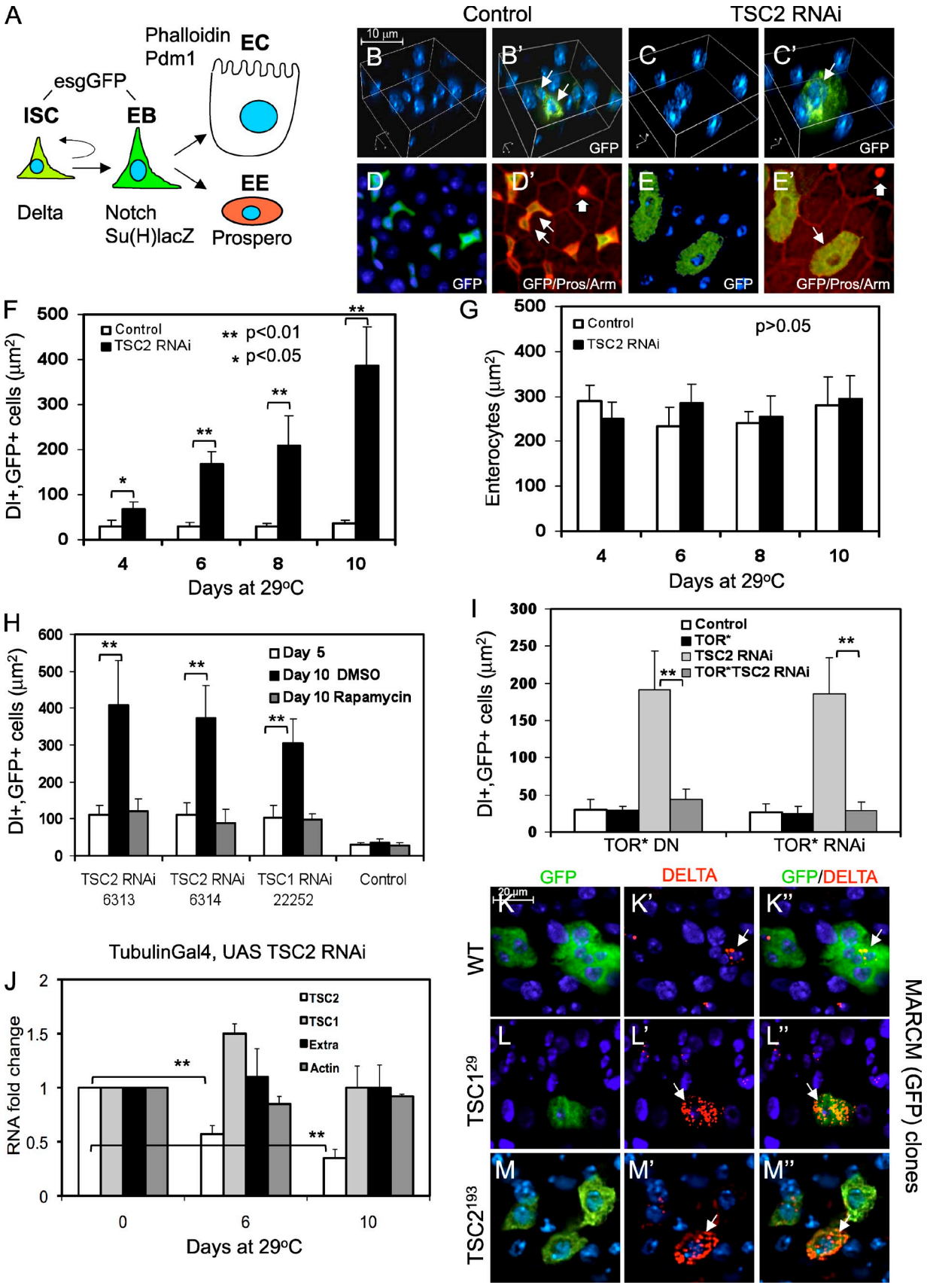

Figure 1. **TSC–TOR regulates ISC growth in the adult midgut.** (A) Cell types in adult midgut. ISC, intestinal stem cell; EB, enteroblast; EE, enteroendocrine cell; EC, enterocyte. Delta, Su(H)-lacZ, Prospero, and fluorescent phalloidin Pdm1 are markers for the indicated cell types. The esg>GFP (> is Gal4-UAS) is expressed in both the ISC and enteroblast. (B–E') 3D reconstruction (B and C) of and normal confocal images (D and E) of control and *TSC2* RNAi cells. The control flies

In addition to the Delta–Notch pathway, recent studies demonstrate that the EGF receptor pathway, Wingless pathway, Decapentaplegic pathway, and intrinsic chromatin modification by the deubiquitinase Scrawny are required for the development and maintenance of ISCs (Lin et al., 2008; Buszczak et al., 2009; Jiang and Edgar, 2009; Lee et al., 2009; Buchon et al., 2010; Mathur et al., 2010; Biteau and Jasper, 2011; Jiang et al., 2011). JNK, p38, and, possibly, PVF2 are required for the regulation of ISCs in aging flies (Biteau et al., 2008; Choi et al., 2008; Park et al., 2009). The insulin receptor (InR), Janus kinase–signal transducer and activator of transcription, Hippo, and JNK signaling are essential for ISC division during homeostasis and pathogenic stimulation (Maeda et al., 2008; Amcheslavsky et al., 2009; Apidianakis et al., 2009; Buchon et al., 2009a,b; Chatterjee and Ip, 2009; Cronin et al., 2009; Jiang et al., 2009; Beebe et al., 2010; Karpowicz et al., 2010; Lin et al., 2010; Ren et al., 2010; Shaw et al., 2010; Staley and Irvine, 2010). Therefore, conserved regulatory pathways are involved in ISC-mediated homeostasis.

In this study, we used an RNAi-based genetic screen to search for important stem cell regulators and have identified tuberous sclerosis complex (TSC) as an essential regulator of midgut ISC growth (in this study, cell growth is measured as an increase in cell size). The human disease TSC is characterized by the appearance of benign tumors in multiple tissues, as the result of mutations in either the *TSC1* or *TSC2* gene (Crino, 2008; Huang and Manning, 2008). The *TSC* gene products form a complex that negatively regulates Rheb and target of rapamycin (TOR). We show here that loss of TSC in midgut ISCs leads to excessive cell growth, which in turn causes defects in ISC division. These stem cell defects lead to a thinner gut epithelium, and the flies have increased susceptibility to feeding of tissue-damaging agents.

Results

ISCs exhibit highly excessive growth in loss of TSC function

To search for essential regulators of ISCs, we used the escargot (esg) Gal4–upstream activation sequence (UAS) system to knock down specific targets by RNAi in adult midgut precursor cells (Fig. 1 A). We included the tubulin-Gal80^{ts} to control temporally double-stranded RNA (dsRNA) expression; at 29°C, the repressor Gal80^{ts} will not be active and will thus allow Gal4 to drive the expression of UAS constructs. The *UAS-mCD8GFP* construct was included to illuminate the affected cells. In control guts, the GFP-positive (GFP+) cells were smaller and frequently in pairs, representing the ISC and enteroblast cell nests in young flies (Fig. 1, B′ and D′, arrow pairs). In *TSC2* dsRNA (Vienna *Drosophila* RNAi Center [VDRC] no. 6313)–expressing guts, the GFP+ cells were much larger and present as individual cells (Fig. 1, C and E). We measured the size of ISCs (Delta+ and GFP+ cells) based on the area in confocal images. The size of the ISCs increased progressively after RNAi initiation to ∼10-fold in 10 d (Fig. 1 F). The surrounding mature enterocytes had no GFP expression (Fig. 1 E′) and did not show any size increase (Fig. 1 G). The enteroendocrine cells were also not affected, as revealed by nuclear staining of Prospero and cell membrane staining of β-catenin/Armadillo (Fig. 1, D′ and E′, thick arrows). Although the esgGal4 driver is expressed in both ISC and enteroblast together with the Delta staining, we demonstrate that loss of TSC2 function induces a substantial increase in cell size in ISCs.

We performed a series of experiments to demonstrate that the well-studied TSC–TOR pathway regulates adult ISCs. TSC is a protein complex that consists of TSC1 and TSC2, and they negatively regulate TOR to control translation and cell growth. Two *TSC2* RNAi lines (VDRC no. 6313 and 6314) and one *TSC1* RNAi line (VDRC no. 22252) all showed a similar size increase (Fig. 1 H). Next, we examined the requirement of TOR by feeding the specific inhibitor rapamycin to the RNAi flies. Administration of rapamycin efficiently suppressed the increase in cell size during RNAi induction (Fig. 1 H). We then used a TOR dominant-negative construct as well as *TOR* RNAi to show that the *TSC2* RNAi-induced size increase is TOR dependent (Fig. 1 I). Therefore, we have demonstrated that the well-studied TSC–TOR pathway regulates cell growth in adult midgut ISCs.

Real-time RT-PCR was used to measure the knockdown efficiency by RNAi. The result revealed an ∼60% decrease of *TSC2* RNA in the whole gut under the tubulin-Gal4 ubiquitous driver (Fig. 1 J). The use of esgGal4 for this experiment would not be as accurate because only the precursor cells in the dissected gut would have the RNAi effect. Although the knockdown

were esg>GFP;tubulin-Gal80^{ts}. The arrows in B′ and D′ indicate pairs of GFP+ cells representing normal ISCs and enteroblasts. The arrows in C′ and E′ indicate single GFP+ cells that have much larger cell sizes. The thick arrows in D′ and E′ indicate Prospero+ enteroendocrine cells that have normal size. For this and other figures, the blue stain is DAPI for nuclear DNA, and the green is GFP unless otherwise indicated. Red membrane staining is Armadillo/β-catenin (Arm), and red nuclear staining is Prospero (Pros). For this and other figures, the scale bar is shown in the first panel and is the same in all other panels within the same image group. (F and G) Quantification of cell size. 29°C incubation would inactivate the Gal80^{ts} repressor to allow Gal4 to function and initiate RNAi. The area in square micrometers of the cells from confocal images for Armadillo staining or GFP was measured, and the data are plotted as the mean. The error bars are standard deviations, and the p-value was obtained from Student's *t* test. (F) $n \geq 30$. (G) $n \geq 62$. (H) Two *TSC2* RNAi lines (VDRC no. 6313 and 6314) and one *TSC1* RNAi line (no. 22252) after RNAi induction for 5 d already exhibit a size increase when compared with the control (white bars). With further incubation until day 10, the DMSO control cells have additional growth (black bars). A similar incubation with rapamycin in the food inhibits additional growth (gray bars). $n \geq 15$. (I) TOR-dependent growth of *TSC2* RNAi midgut cells. The TOR* construct was either a TOR dominant negative (DN) or *TOR* RNAi, both of which were under the control of the UAS. The expression of either construct alone for 6 d had no effect on growth but efficiently suppressed the growth induced by *TSC2* RNAi. $n \geq 24$. (J) *TSC2* dsRNA was expressed in the gut using the tubulin-Gal4;tubulin-Gal80^{ts} combination. RT–quantitative PCR was performed to assess the relative levels of *TSC2*, *TSC1*, *extra* (CG6634), and *actin* RNA at 0, 6, and 10 d after RNAi initiation at 29°C. Three independent RNA isolations were performed, and each PCR included duplicated samples. (K–M″) MRACM clonal analysis of *TSC* mutants. Flies with the indicated genotypes were heat shocked at 37°C to induce mitotic recombination that produced GFP+ mutant cells. After heat shock, the flies were incubated at 29°C, and the guts were dissected after 6 d. The wild-type (WT) chromosome gave rise to clusters of GFP+ cells, with one of the small cells showing Delta staining (indicated by arrows), presumably the parental ISC. The mutant *TSC* cells that were GFP+ and contained Delta staining (arrows) remained as single cells but increased in size in older flies. Dl, Delta.

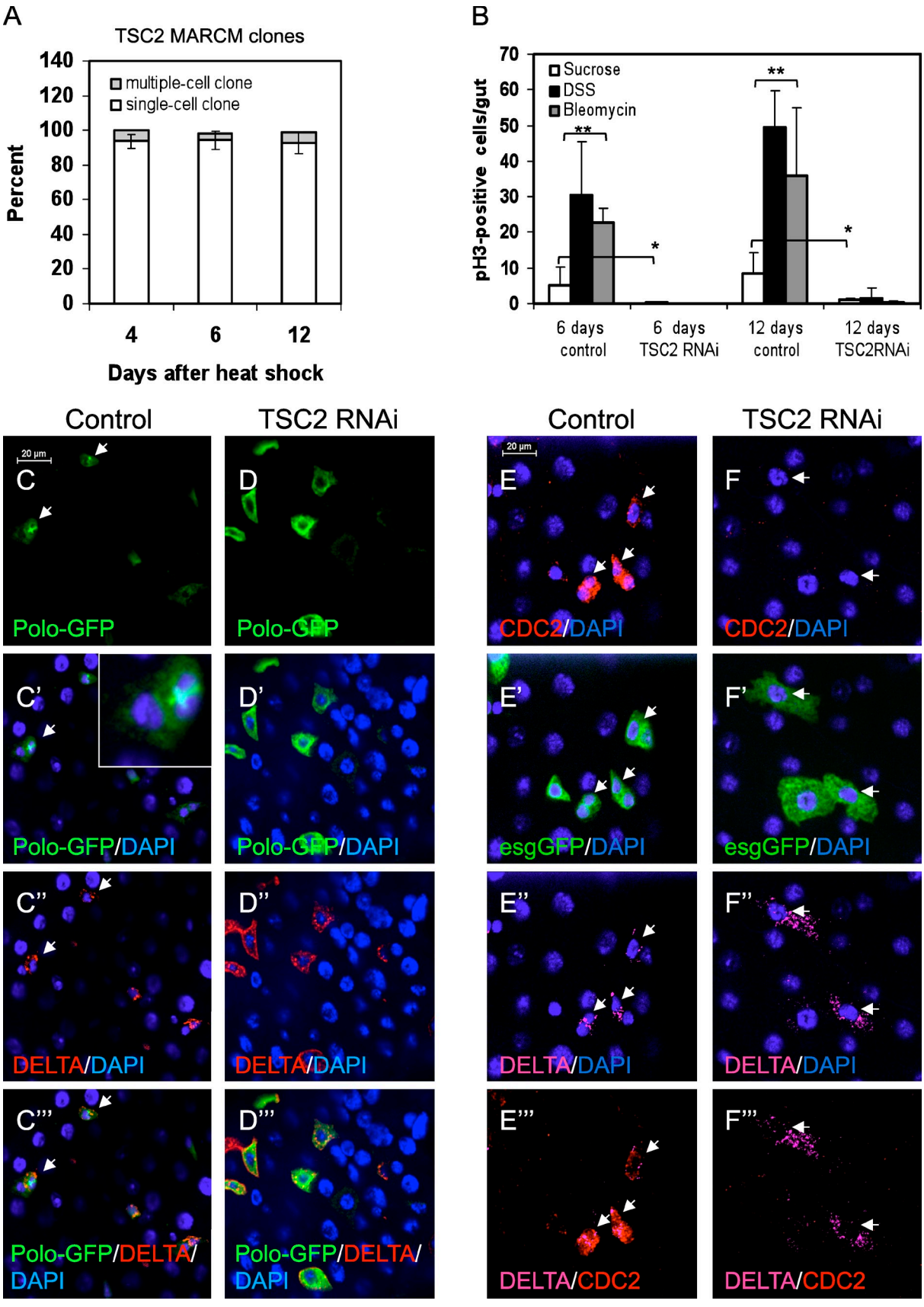

Figure 2. **Loss of TSC causes defects in mitotic regulators and ISC division.** (A) The number of days after heat shock induction of mitotic recombination in *TSC2*^{193} mutant MARCM flies is indicated. The guts were stained for Delta. GFP+ clusters or single cells that also contained Delta were counted. If a cluster contained two or more GFP+ cells, it was counted as a multiple-cell clone. Most Delta+ MARCM cells remained as single cells. $n \geq 175$. (B) The *TSC2* RNAi was v6313 crossed

appeared to be specific, and the RNAi-induced cell growth phenotype was consistent with the known function of TSC, we confirmed the phenotypes by mosaic analysis with repressible cell marker (MARCM; Lee and Luo, 2001; Amcheslavsky et al., 2009). Three *TSC2* mutant alleles were tested: $TSC2^{56}$, which is a weak allele, and $TSC2^{192}$ and $TSC2^{193}$, which are null alleles (Ito and Rubin, 1999). The staining of these guts with Delta together with the GFP marking showed that all the *TSC2* mutants caused an increased ISC size between day 4 and 12 after the heat shock regimen (Fig. 1 M, $TSC2^{193}$ allele). This increase in ISC size was also observed with $TSC1^{12}$ and $TSC1^{29}$ alleles (Fig. 1 L, $TSC1^{29}$ allele) but not with wild-type chromosomes (Fig. 1 K). We conclude that TSC loss of function causes cell-autonomous growth of ISCs in the adult midgut.

Loss of TSC causes defects in ISC division

TSC has been dubbed a tumor suppressor because previous studies have shown that *TSC* mutant cells have increased cell division in addition to cell growth (Ito and Rubin, 1999; Gao and Pan, 2001; Tapon et al., 2001; Rosner et al., 2006; Huang and Manning, 2008). However, our observations suggest a major deviation from the current paradigm, such that loss of TSC in adult *Drosophila* ISCs leads to a halt in cell division. First, MARCM analysis revealed that most *TSC2* mutant cells that were also Delta+ grew larger but remained as individual cells without clonal expansion (Fig. 2 A and Fig. 1 M), whereas wild-type ISCs formed GFP clones with many more cells (Fig. 1 K). Similar results were observed with the *TSC1* mutant clones (Fig. 1 L). Second, the *TSC2* RNAi guts had a reduction in phosphorylated histone 3–positive (pH3+) cells (Fig. 2 B, white bars). ISCs are the only mitotic cells within the adult midgut, and pH3 staining reveals ISCs that are in mitosis. Third, when the flies were fed with tissue-damaging agents dextran sulfate sodium (DSS) and bleomycin, the number of pH3+ cells increased in the wild-type guts but not in *TSC2* RNAi guts (Fig. 2 B, black and gray bars). Together, these results demonstrate that *TSC* mutant ISCs do not divide.

We further analyzed the cell division phenotype by examining the expression of specific regulators. The kinase Polo is essential for mitosis and meiosis and is localized in different compartments at different phases of the cell cycle (Llamazares et al., 1991). By using a fusion protein trap line (FlyTrap no. CC01326), we found that Polo-GFP was detectable in Delta+ cells. Similar to a previous study (Llamazares et al., 1991), the Polo-GFP fusion protein was, at times, highly concentrated at the ISC metaphase plate (Fig. 2, C and C′). In wild-type guts, 3.0% (16/538) of the Polo-GFP–positive cells had this metaphase pattern, which likely represents the number of ISCs undergoing mitosis. In the *TSC2* RNAi gut, the Polo-GFP was still clearly detectable as cytoplasmic staining (Fig. 2 D), but only 0.2% (2/843) of the cells showed the metaphase staining pattern.

Another essential component for mitotic entry is the kinase Cdc2 (Royou et al., 2008). Our staining data show that in wild-type guts, Cdc2 is expressed in all Delta+,esg>GFP+ (> is Gal4-UAS; Fig. 2, E–E‴, arrows) but only in some Delta−,esg>GFP+ cells. Therefore, Cdc2 is most likely expressed in ISCs and segregated into newly formed enteroblasts. In *TSC2* RNAi guts, we could not detect any Cdc2 staining in any of the cell types (Fig. 2, F–F‴). The loss of Cdc2 supports the observation that *TSC2* mutant ISCs have division defects.

TSC mutant ISCs have additional defects during S phase

The aforementioned results show that the mutant cells grow bigger and do not divide, raising the possibility that these cells may undergo endoreplication if DNA synthesis is normal. We performed 5-ethynyl-2'-deoxyuridine (EdU) feeding and incorporation experiments to examine whether the *TSC2* RNAi or mutant cells are normal in S phase. The traditional BrdU incorporation/detection is not as sensitive as EdU (Staley and Irvine, 2010) and requires feeding time of a few days, which leads to a difficult interpretation of results. Therefore, we developed an EdU feeding protocol that allowed us to perform a much shorter feeding time of 6–24 h and gave better snapshots of the replication activity at various time points after RNAi initiation. We show in Fig. 3 the 24 h feeding results, which clearly indicate that the number of Delta+ cells that had detectable EdU incorporation was significantly reduced, especially in day 6 and day 8 (Fig. 3 A). We also performed MARCM clonal experiments using a null *TSC2* mutant allele, and the result showed that most of these null cells had no detectable incorporation (Fig. 3 B).

To investigate the cell cycle defects further, we performed a tissue dissociation and cell-sorting experiment. Dissected guts were incubated with trypsin to release gut cells into suspension, which were stained with Hoechst 33342 DNA dye and analyzed by FACS. The esg>GFP control guts gave 11.3% of cells that had a strong GFP signal (Fig. 4 A, boxed area), whereas the *TSC2* RNAi guts gave a lower percentage (6.86%) in the same gated area (Fig. 4 B), which is consistent with the mutant ISCs being unable to divide. The wild-type GFP-positive cells showed tight DNA dye profiling (Fig. 4 C), and computer modeling suggested that 82% of the cells were 2N or in G1 (Fig. 4 C′). As a comparison, the overexpression of Myc drives more cells to completion of S phase (Johnston et al., 1999; Wu and Johnston, 2010), resulting in a profile that had clearly distinguishable 2N and 4N peaks (Fig. 4, D and D′). Meanwhile, cells from *TSC2*

with the esg>GFP;tubulin-Gal80^{ts} flies. The control guts had ∼5–10 mitotic cells after 6 or 12 d of incubation at 29°C, whereas the *TSC2* RNAi guts had almost no detectable mitotic cells after a similar incubation (white bars). Feeding of DSS or bleomycin increased the mitotic cell counts in the control flies, but similar feeding could not increase mitotic cell counts in the *TSC2* RNAi flies. Three independent experiments were performed, and four guts were counted for each sample. (C–D‴) The Polo-GFP is a protein trap line. The expression was detected by anti-GFP immunofluorescent staining. Most Polo-GFP+ cells also had Delta staining. In some wild-type cells, the GFP fusion is enriched at the metaphase plate (arrows in C–C‴ and inset in C′). In *TSC2* RNAi flies, the Polo-GFP was still detectable in the cytoplasm of Delta+ cells, but almost none of them showed metaphase plate staining. (E–F‴) The control was esg>GFP, and Cdc2 and Delta antibodies were used for immunofluorescent staining. The arrows in these panels indicate Delta+ cells. In control guts, all Delta+ cells also had Cdc2 staining. In *TSC2* RNAi guts, the esg>GFP+;Delta+ cells were larger, but they did not contain Cdc2 staining. Error bars are standard deviations. *, $P < 0.05$; **, $P < 0.01$.

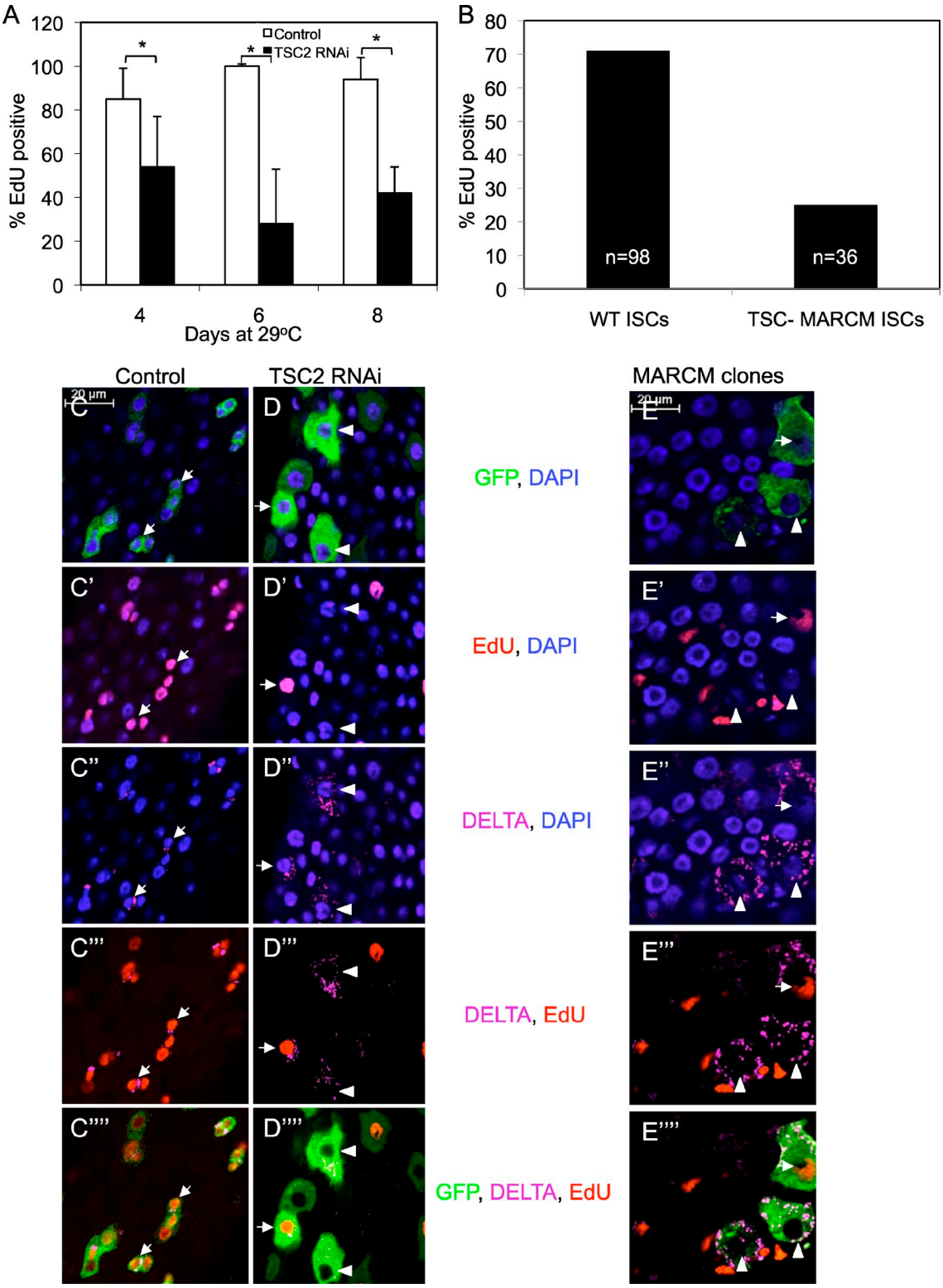

Figure 3. ***TSC2* mutant ISCs had reduced DNA replication.** (A) The esg>GFP control and *TSC2* RNAi flies were incubated in 29°C for a total of 4, 6, or 8 d. EdU was added to a 5% sucrose solution for feeding flies for 24 h in the final day. Guts were dissected and used for Delta antibody staining and EdU detection using the Click-iT detection kit. GFP+;Delta+ cells were counted, and the percentage of them that also had an EdU signal is plotted as shown. Using this feeding protocol, 80–100% of Delta+ cells in control guts also contained an EdU signal. In *TSC2* RNAi guts, only 30–50% of Delta+ cells contained an EdU signal. $n \geq 75$. (B) *TSC2* mutant MARCM clones were induced by heat shock, returned to 29°C for 5 d, and then fed with EdU for 1 d. MARCM GFP+ cells that were also Delta+ were counted as total number of cells; 25% of them also had EdU staining. The wild-type (WT) ISCs were the Delta+ cells that surround the MARCM ISCs; 71% of which showed EdU staining. (C–E′′′′) Confocal images of staining for control, *TSC2* RNAi, and *TSC2* mutant MARCM guts. In C–C′′′′, most esg>GFP+ and Delta+ (arrows) control cells were small and had EdU incorporation. In D–D′′′′, most *TSC2* RNAi Delta+ cells did not have EdU (arrowheads), but some still can incorporate (arrows). In E–E′′′′, most *TSC2* mutant MARCM cells that were Delta+ did not show EdU staining (arrowheads), whereas a few did (arrows). Error bars are standard deviations. *, $P < 0.05$.

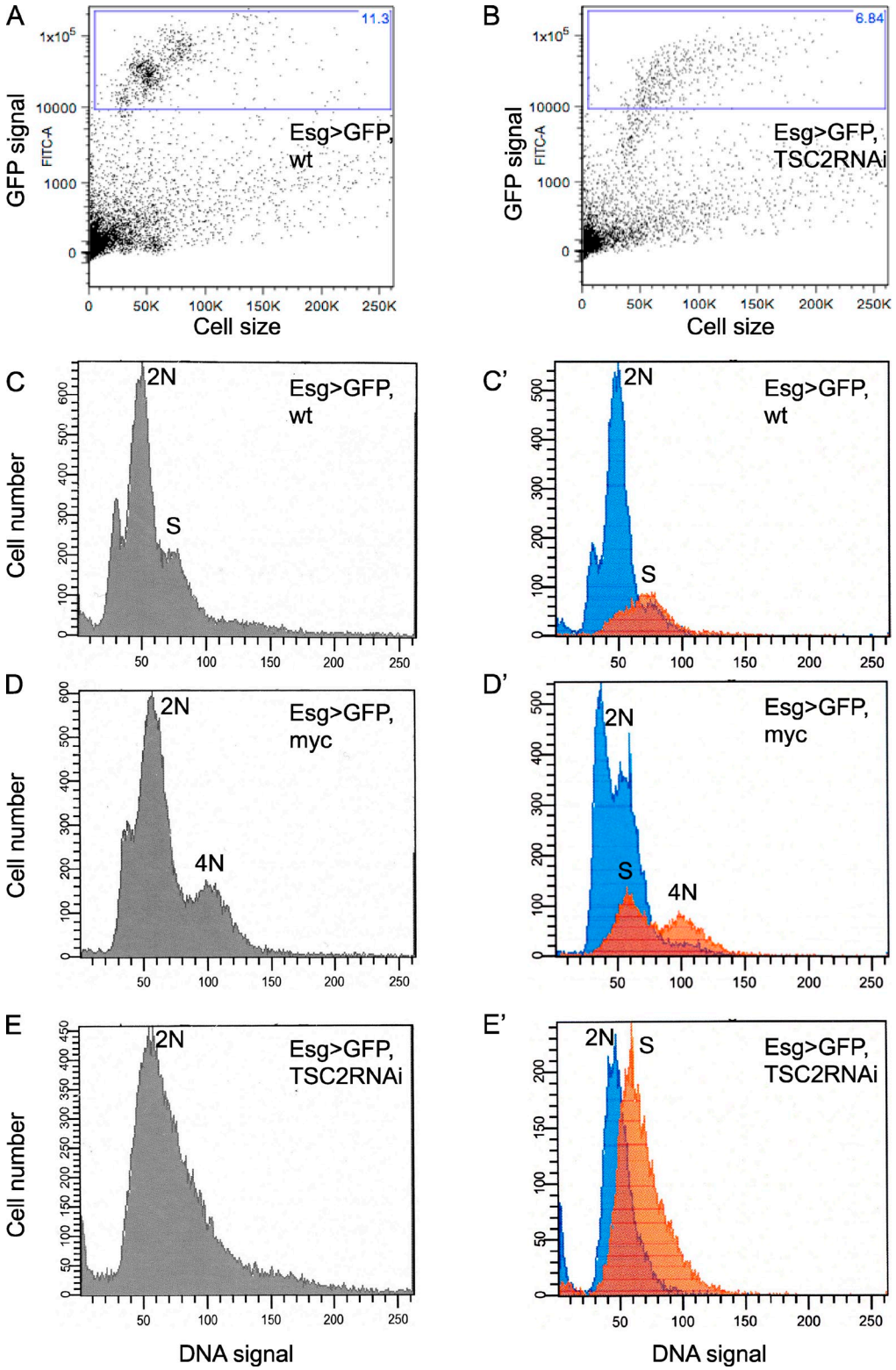

Figure 4. **TSC2 mutant cells had defective S-phase progression.** (A and B) FACS analysis of dissociated gut cells. When control esg>GFP fly gut cells were analyzed, 11.3% of the count showed a strong GFP signal (boxed area in A). Cells with similar GFP signals were analyzed in *TSC2* RNAi fly guts (boxed area in B, 6.84%). These cells spread toward the right, which is consistent with an overall increase in cell size. Control w^{1118} fly gut cells did not show any GFP signal in the similarly boxed area (not depicted). (C and C′) The GFP-positive cells in the boxed area of the control guts used for DNA dye profiling showed clustering into a major peak and a minor peak, which should correspond to 2N and S-phase cells, respectively. C′ is a computer model for contribution from G1 (2N)- and S-phase cells. (D and D′) Cell cycle profiling in guts overexpressing Myc. In this condition, a 4N peak is clearly observed, which is consistent with published results showing that Myc can drive cells through S phase, and therefore, more cells have 4N DNA content. D′ is the computer model for contribution from 2N, S, and 4N cells. (E and E′) GFP+ cells from *TSC2* RNAi guts showed a broader distribution, which peaked near 2N but spread toward 4N. E′ is the computer model suggesting that a much higher percentage of cells were in S phase. wt, wild type.

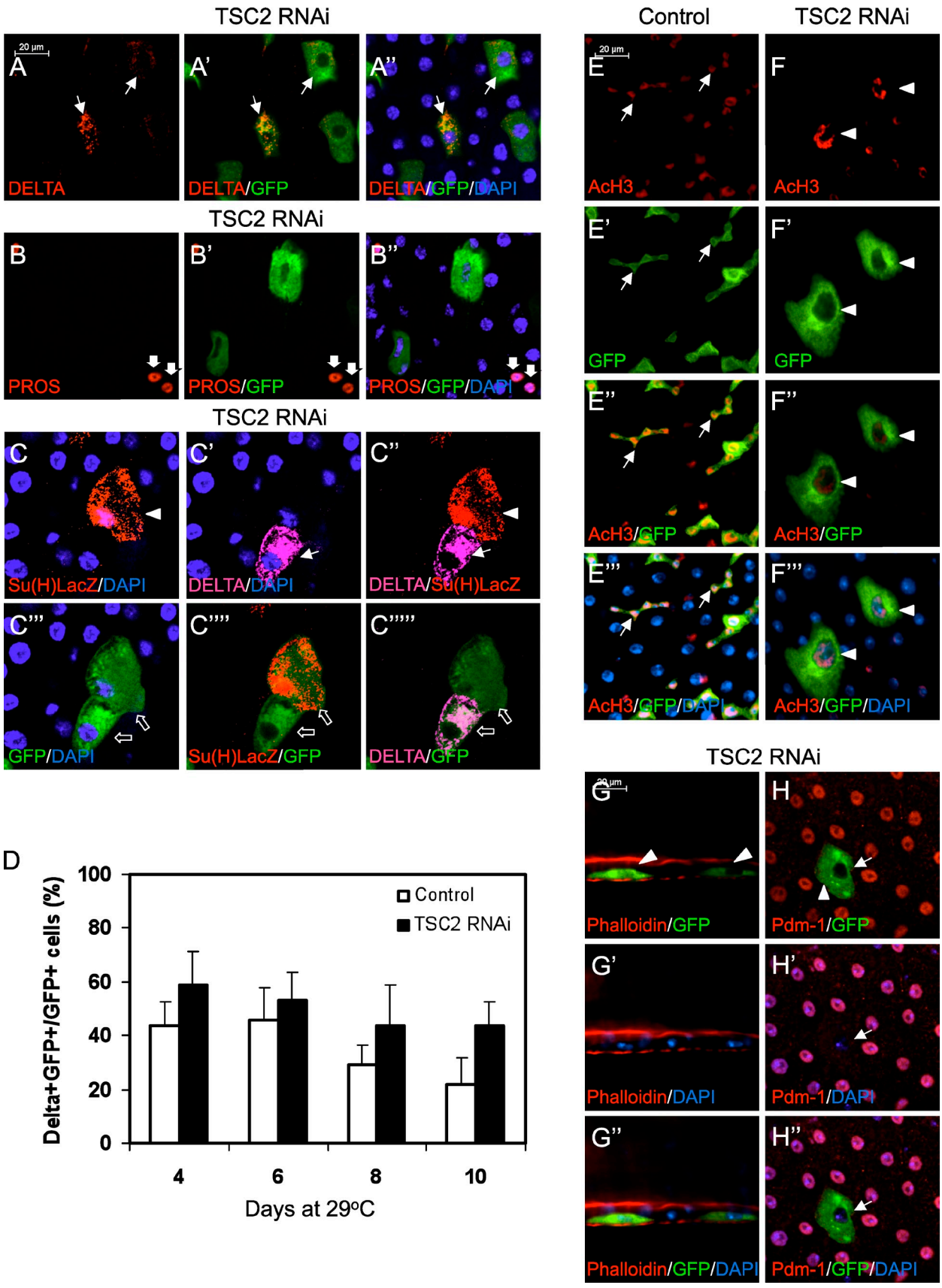

Figure 5. **ISCs without TSC2 function still express correct cell fate markers.** (A–C'''') The esg>GFP;tubulin-Gal80^{ts} line was crossed with the *TSC2* RNAi (6313) line and the offspring was incubated at 29°C for 8 d before dissection. Many of the esg>GFP+ cells also contained Delta (A–A'', arrows). Therefore, these cells express two markers that define ISC. The esg>GFP+ cells did not express Prospero (PROS), which was present in enteroendocrine cells

RNAi guts showed a broader profile but did not form another peak (Fig. 4 E). Computer modeling suggested that ∼65% of these cells had DNA content between 2N and 4N (Fig. 4 E′). This result suggests that many *TSC2* RNAi cells can enter S phase but either stop or slow down, leading to the accumulation of different amounts of DNA in the population.

Based on both the EdU incorporation and FACS analysis, we conclude that *TSC2* RNAi midgut precursor cells have significantly slower DNA synthesis and do not have synchronized S phase. However, because mitosis is abolished, even slow DNA replication over time will cause polyploidy in these large mutant cells. This will be different from mutant imaginal disc cells, which continue to divide and, therefore, have a modest size increase and remain diploid (Ito and Rubin, 1999; Gao and Pan, 2001; Tapon et al., 2001). Our FACS analysis of *TSC2* RNAi cells at later time points did show an even broader profile. However, because of the extreme cell size increase, the DNA signal comparison between small control cells and large mutant cells becomes unreliable. Therefore, we speculate that the large mutant cells in the adult midgut are not in active endoreplication, although they have DNA content larger than 2N because of the lack of cell division and slow DNA synthesis.

Loss of TSC allows cell growth but does not direct differentiation

When an ISC divides, two cells are formed with one becoming a renewed ISC and the other becoming an enteroblast. The enteroblast ceases to divide and starts to differentiate, which is associated with substantial growth if committing to the enterocyte lineage (Fig. 1 A). Therefore, the aforementioned *TSC* mutant phenotypes can be a result of directed differentiation. However, the detection of both Delta and *esg>GFP* (Fig. 5 A, arrows), two major stem cell markers in adult *Drosophila* ISCs, in many of the large *TSC* mutant cells suggests that they have retained at least some stem cell properties. Therefore, we next performed analyses of various makers to determine whether these mutant ISCs are largely undifferentiated. As shown in Fig. 5 B, staining of the large GFP+ cells with Prospero was negative, whereas the small enteroendocrine cells stained positive for this marker (Fig. 5 B, thick arrows). In addition, the Delta and the Notch pathway target gene *Su(H)-lacZ* stained separate cells when two occasional neighboring cells both had esg>GFP expression (Fig. 5, C–C′′′′). Therefore, the ISC versus enteroblast fate has been maintained after *TSC2* RNAi. We also quantified the relative number of Delta+ cells over the experimental period. In wild-type flies, progressively older fly guts had a decreasing Delta+ to esg>GFP+ cell ratio, from ∼40 to 20% (Fig. 5 D, white bars). This reflects the accumulation of more enteroblasts after divisions during which the ISCs are renewed but not increased. If there is ISC loss, we expect this ratio will decline faster. In *TSC2* RNAi guts, the ratio declined from ∼60 to 50% (Fig. 5 D, black bars). This is consistent with no cell division, and there is also no indication of stem cell loss after *TSC2* RNAi.

The stem cell state and subsequent differentiation are often correlated with specific chromatin modifications (Boheler, 2009; Buszczak et al., 2009; Sang et al., 2009). In wild-type guts, we observed that precursor cells marked by *esg>GFP* exhibited a more prominent nuclear staining of acetylated histone 3 (AcH3; Fig. 5 E, arrows). Importantly, the large *TSC2* RNAi cells also exhibited this stronger AcH3 nuclear staining (Fig. 5 F, arrowheads), suggesting that they were precursor-like cells. Fluorescent phalloidin illuminates F-actin present at the apical brush border of mature enterocytes and in smooth muscle cells (Micchelli and Perrimon, 2006; Amcheslavsky et al., 2009). We found that >90% of the large GFP+ cells examined after 8 d of RNAi treatment showed no direct overlap with phalloidin staining (Fig. 5 G, arrowheads). The POU domain protein Pdm1 is a newly identified mature enterocyte marker (Bardin et al., 2010). We stained for Pdm1 and found that it was not expressed in the big *TSC2* RNAi cells but was clearly present in surrounding enterocytes (Fig. 5 F). Therefore, ISCs that have lost TSC2 function remain undifferentiated.

TSC coordinates ISC growth and division through TORC1 but not TORC2

We conducted additional experiments to gain further insight into the mechanism by which TSC regulates ISC division. In cases in which InR acts directly upstream, it usually suppresses TSC function (Pan et al., 2004; Avruch et al., 2006), and thus, InR and TSC have opposite functions and should exhibit opposite phenotypes. However, in ISCs, loss of InR and loss of TSC both abolish division, which is also observed in germline stem cells (Amcheslavsky et al., 2009; Hsu and Drummond-Barbosa, 2009). Furthermore, administration of rapamycin only modestly suppressed InR-stimulated ISC division (Fig. 6 A). Therefore, it is unlikely that InR signaling simply represses TSC to allow TOR to stimulate division in ISCs. We next simultaneously inactivated TSC by *TSC2* RNAi and activated the InR pathway either by expressing an activated InR or by RNAi knockdown of *PTEN*, a negative regulator of the InR pathway. As shown in Fig. 6 B, ∼80% of the InR-stimulated or *PTEN* RNAi–induced mitotic activity was suppressed by loss of TSC function.

(B–B″, thick arrows). Occasionally, the large esg>GFP+ cells were present as a pair; within this pair, one expressed the enteroblast marker Su(H)-lacZ, and the other expressed Delta (arrowheads and arrows, respectively, in C–C″). In C‴–C′′′′, arrows indicate GFP+ cells. (D) Quantification of Delta+ cells in *TSC2* RNAi guts. The fly guts, as described previously in this paragraph, were used for confocal image analysis, and the numbers of Delta+ and esg>GFP+ cells were counted. The number of Delta+ cells over the total number of GFP+ cells is expressed as a percentage and plotted. $n \geq 207$. (E–F″) A higher level of acetylated histone 3 (AcH3) staining was associated with small nuclei in the control guts (arrows are two examples). This nuclear staining overlapped with the esg>GFP, indicating that AcH3 staining is higher in precursor cells. In *TSC2* RNAi guts, the large esg>GFP cells also contained a higher level of AcH3 (arrowheads). Therefore, these large cells retained a precursor cell property. (G–G″) Fluorescent phalloidin was used to stain *TSC2* RNAi guts. The actin brush border in enterocytes, and the underlying smooth muscle had a high level of fluorescent phalloidin signal. The large esg>GFP+ cells did not overlap with the fluorescent phalloidin signal (arrowheads indicate the gap). (H–H″) Pdm1 was detectable in the nuclei of mature large cells, the enterocytes. However, the large esg>GFP+ cells in which *TSC2* RNAi was expressed (arrows) did not have detectable Pdm1 staining. The arrowhead indicates a large GFP+ cell that has no nuclear Pdm1 staining. Error bars are standard deviations.

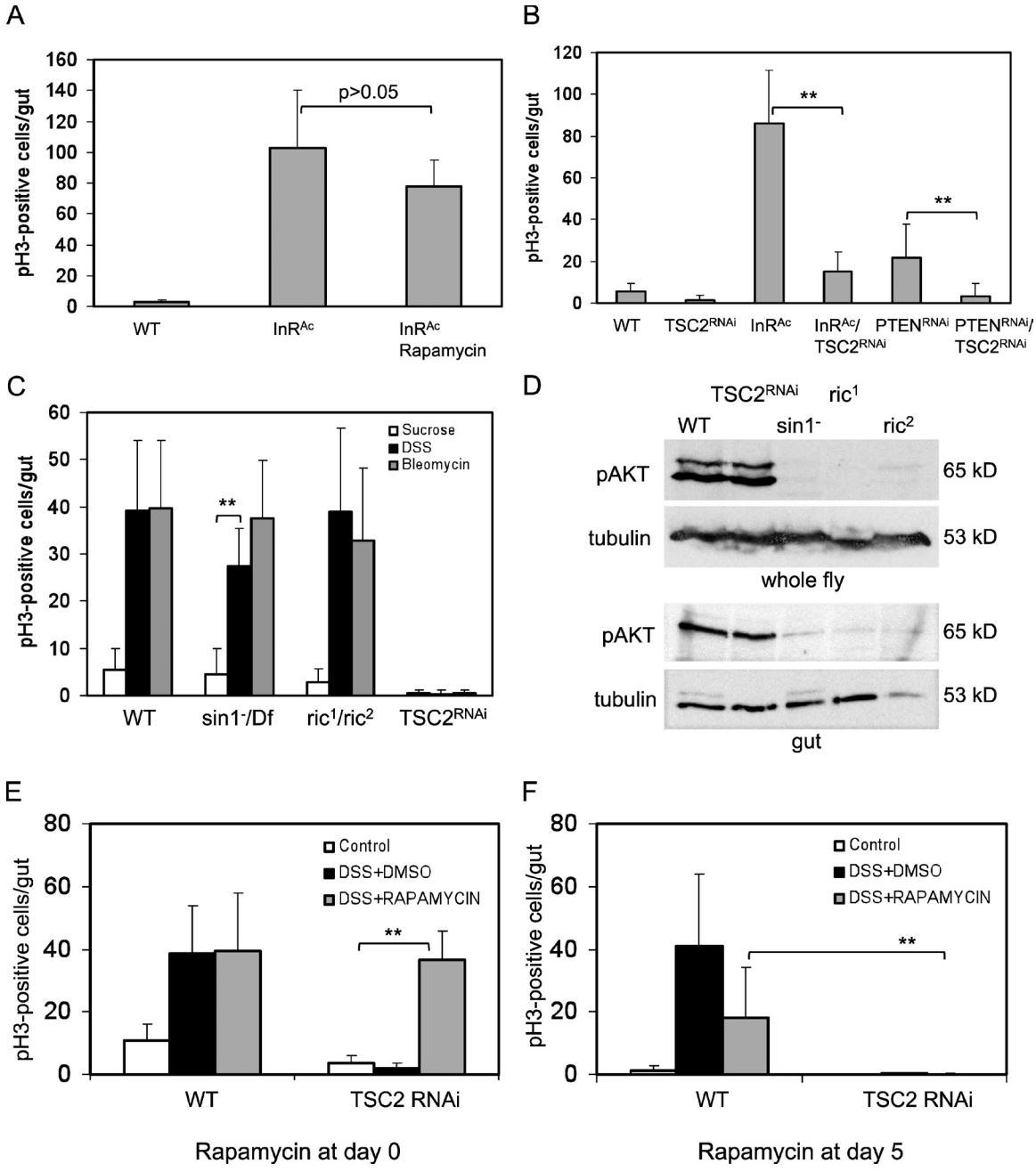

Figure 6. **TSC regulates ISC growth and division through TORC1 but not TORC2.** (A) Expression of InR^{Ac} (InR^{A1325D}) by the esgGal4 driver increased pH3 count. Feeding of rapamycin decreased the pH3 count by only a small fraction. $n = 10$. (B) Expression of InR^{Ac} or *PTEN* RNAi driven by esgGal4 increased pH3 count by ~10- and 4-fold, respectively. *TSC2* RNAi suppressed the pH3 count in the midguts of wild-type (WT), InR^{Ac}, and PTEN RNAi flies. $n \geq 12$. (C) The pH3 count in wild-type and mutant guts with or without feeding tissue-damaging agents (DSS and bleomycin). The wild-type, *sin1*/deficiency, and *ric1/ric2* fly guts all showed an increase in pH3 count after tissue damage. In contrast, the *TSC2* RNAi fly guts showed highly reduced mitotic count in all conditions. Four independent experiments were performed, and four guts were examined for each sample. (D) Western blots showing the C-terminal phosphorylation of AKT in various genetic backgrounds. There was a substantial reduction of AKT phosphorylation in *sin1* and *rictor* mutant flies and guts. However, the *TSC2* RNAi flies and guts showed similar AKT phosphorylation as wild type. The *TSC2* RNAi was driven by the esgGal4. (E) esg>GFP;tubulin-$Gal80^{ts}$ flies were used as wild type. Feeding with DSS increased the pH3 count, whereas inclusion of DMSO or rapamycin in the food did not change the mitotic count in wild-type flies. Similar feeding experiments with *TSC2* RNAi flies showed that adding rapamycin at the beginning of the experiment (day 0) restored the mitotic activity. (F) A similar rapamycin and DMSO feeding experiment as in E with the exception that the rapamycin and DMSO were included in the food at day 5 after shifting the temperature to 29°C to initiate the *TSC2* RNAi. This late rapamycin treatment did not restore the pH3 count. (E and F) Three independent experiments were performed, and four guts were examined for each sample. Error bars are standard deviations. **, $P < 0.01$.

This genetic suppression implies that TSC acts in parallel or downstream of InR/PTEN but is a positive regulator of ISC division. In consideration of all the results, we surmise that InR and TSC act in parallel to regulate ISC division (see Fig. 8 E).

Recent evidence suggests that TSC can regulate two different TOR complexes: TORC1 and TORC2 (Huang and Manning, 2009; Inoki and Guan, 2009). In the canonical pathway, TSC represses TORC1 by acting as a GTPase-activating protein for

the GTPase Rheb. In the second pathway, TSC may activate TORC2 independently of the GTPase-activating protein activity (Huang et al., 2009). TORC2 contains two distinct components called Sin1 and Rictor (Sarbassov et al., 2005; Guertin et al., 2006). Therefore, we examined ISC division in the genetic mutants of *sin1* and *rictor*, both of which are viable strains (Hietakangas and Cohen, 2007). We found that these mutants behaved similarly to wild-type flies in basal or damage-stimulated ISC division (Fig. 6 C). One observed defect in the *sin1* and *rictor* mutants is a lack of AKT phosphorylation at the C terminus, which enhances AKT activity in conjunction with InR signaling (Sarbassov et al., 2005; Guertin et al., 2006; Hietakangas and Cohen, 2007). This lack of C-terminal AKT phosphorylation was readily detectable in whole fly and gut extracts of the *sin1* and *rictor* mutants (Fig. 6 D). However, the *TSC2* RNAi guts showed a normal level of AKT phosphorylation. Therefore, loss of ISC division in *TSC* mutant guts is not caused by deregulation of the TORC2 pathway.

Two other possible mechanisms are that TSC2 regulates ISC division through an unknown pathway or through TORC1, which causes excessive growth that may block cell division. Rapamycin is a potent inhibitor of TORC1. We therefore used this chemical to examine the effect of TORC1 inhibition on cell division in *TSC2* RNAi guts. Rapamycin was fed either at the beginning of RNAi induction (day 0) or at the time 5 d after RNAi initiation (day 5). The experiment was continued for a total of 10 d, and DSS was added during the last 2 d to stimulate cell division. When rapamycin was given at the beginning of the experiment, the *TSC2* RNAi–induced growth increase and division defect were both suppressed (Fig. 6 E). However, if *TSC2* RNAi was allowed to take effect for 5 d, which causes the ISCs to grow by approximately fourfold (Fig. 1), rapamycin administration could not rescue the ISC division defect (Fig. 6 F), despite suppressing further growth. Therefore, by inhibiting growth right at the beginning, the size of the ISCs remained normal, and they were able to divide even in the absence of TSC2. These results suggest that the ISC division defects observed in the *TSC2* mutant are not because of another pathway but are caused by the excessive growth mediated by TORC1.

Reducing growth by inhibiting Myc can rescue ISC division

To gain further support for the model that excessive growth in ISCs is the reason for the observed inhibition of cell division, we sought other regulators that could inhibit ISC growth. Myc has been shown to regulate cell growth during *Drosophila* development (Johnston et al., 1999; Wu and Johnston, 2010). Overexpression of *Drosophila* Myc in the midgut by the esg-Gal4 driver did not cause a detectable change in cell growth even after 2 or 6 d at a permissive temperature (Fig. 7 A). Nonetheless, the higher level of Myc significantly enhanced the cell growth phenotype induced by *TSC2* RNAi within 2 d (Fig. 7 A), demonstrating that Myc is indeed a growth regulator in the midgut. We then tested the loss of function of *Myc* by esgGal4-driven RNAi. Over a short duration of 2 d, the *Myc* RNAi did not cause a significant change in ISC growth or division (Fig. 7, A and B). However, the *Myc* RNAi, for 6 d or longer, did cause

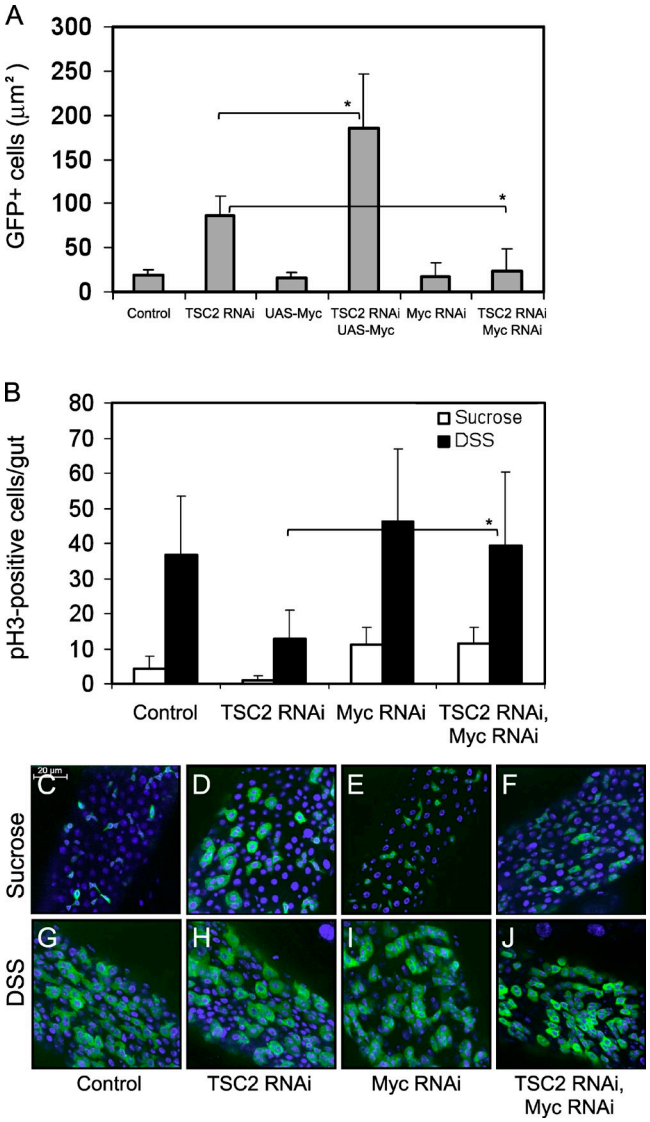

Figure 7. **Myc and TSC coordinate ISC growth and division.** (A) The various transgenic lines were crossed with the control esg>GFP;tubulin Gal80^{ts} line as indicated. The resulting flies were incubated at 29°C for 2 d, and the guts were dissected for microscopy and cell size measurement. $n \geq 43$. (B) The individual and combination RNAi lines were crossed with the control line. The flies were hatched at room temperature and fed sucrose or DSS for 2 d at 29°C. Guts were dissected and stained for pH3 and quantified as shown. $n \geq 20$. (C–J) Confocal images of the control and indicated RNAi lines after sucrose or DSS feeding for 2 d at 29°C. The *TSC2* RNAi cells in both feeding experiments remained large. The *Myc* RNAi cells were similar to the control. The *Myc;TSC2* double RNAi cells were smaller and had more GFP+ cells after DSS feeding. Error bars are standard deviations. *, $P < 0.05$.

a halt of division (unpublished data). We cannot distinguish whether prolonged loss of Myc function affects ISC division directly or the lack of cell growth affects division indirectly. Nevertheless, we used the short duration protocol to inhibit the cell growth phenotype induced by *TSC2* RNAi. Flies that had both *TSC2* RNAi and *Myc* RNAi showed a cell size more similar to that of the control, which was smaller than *TSC2* RNAi samples (Fig. 7, A [right-most sample] and F). These double RNAi flies also exhibited a mitotic index similar to that of the control (Fig. 7 B). Moreover, cell division in these flies in response to DSS feeding

was equal to the control (Fig. 7 B, black bars). The GFP-positive cell number and size were also consistent with the mitotic index (Fig. 7, C–J). Therefore, a reduction in growth by reducing Myc activity can restore ISC division. Together, these results support the hypothesis that the excessive growth in the *TSC* mutant blocks cell division and that, in normal guts, TSC and Myc function to coordinate ISC growth and division.

Loss of TSC leads to increased susceptibility to intestinal damage

To assess the biological outcome in the absence of TSC function within ISCs, we examined the midgut organization by tissue sectioning. The wild-type midgut showed protrusions of mature enterocytes lining the lumen, which was consistent with their normal absorptive functions (Fig. 8 A). However, in *TSC2* RNAi guts, the epithelial layer appeared to be thinner and smoother (Fig. 8 B). Nevertheless, the epithelium still appeared as a continuous sheet.

We then fed the *TSC2* RNAi flies with tissue-damaging agents. DSS and bleomycin feeding causes different damages in the midgut and can kill flies in a dose-dependent manner (Amcheslavsky et al., 2009). When a low dose of 1% DSS in sucrose solution was given, ∼78% of the wild-type flies were still alive at the end of 7 d. However, under the same conditions, only 30% of the *TSC2* RNAi flies were alive at the end of 7 d (Fig. 8 C). Similarly, when a low dose of 2 µg/ml bleomycin was administered for 7 d, 80% of the wild-type flies survived, whereas only 40% of the *TSC2* RNAi flies survived under the same conditions (Fig. 8 D). The increased susceptibility to tissue damage observed in these *TSC2* RNAi flies is consistent with the loss of ISC division, which would lead to fewer precursor cells being available for repair.

Discussion

In this study, we have provided evidence demonstrating that TSC is an essential regulator of ISC growth and division. In the absence of TSC function, ISCs have unrestricted cell growth, which halts cell division and leads to the formation of extremely large cells. Although stem cell markers are still expressed, these ISC-like cells are nonfunctional and can no longer divide or differentiate. As a consequence, the *TSC* mutant gut has a thinner epithelium and the mutant fly is more susceptible to tissue-damaging agents. Our study has uncovered a tissue context–dependent phenotype of TSC mutants, such that unrestricted cell growth can lead to a stop of cell division, and thus, TSC does not function all the time as a classical tumor suppressor.

The TSC–TOR and other growth regulatory pathways, such as InR and Myc, have intricate interactions. Some suggest that the InR pathway directly represses TSC, whereas others and our study here suggest that the two pathways act in parallel (Fig. 7 E; Pan et al., 2004; Avruch et al., 2006). The TSC–TOR pathway also has a negative feedback into upstream components of the InR pathway (Huang and Manning, 2009; Inoki and Guan, 2009). Recent identification of TORC2 in addition to the original TORC1 further complicates these pathways (Hietakangas and Cohen, 2007; Guertin et al., 2009). However, our results clearly show that *TORC2* mutants and *TSC* mutants have different phenotypes in the adult *Drosophila* midgut, suggesting that TSC does not function through TORC2 to regulate ISC division. Previous studies have demonstrated that Myc can modulate TSC–TOR in controlling the growth of mammalian and fly cells (Tapon et al., 2001; Teleman et al., 2008; Schmidt et al., 2009), which is consistent with what we have observed.

In normal development and adult tissue homeostasis, cells need to grow in size by approximately twofold before they divide to maintain the original cell size. Reduction in cell growth below a certain threshold can lead to a halt of division (Grewal and Edgar, 2003; Jorgensen and Tyers, 2004; Leevers and McNeill, 2005). Therefore, the balance between cell growth versus division is a complex process requiring delicate coordination (Kohlmaier and Edgar, 2008). Here, we have shown that, in *TSC* mutants, the increase in midgut ISC size is >10-fold (Fig. 1 and Fig. 2), whereas the increase in larval disc cell size is less than twofold (Ito and Rubin, 1999; Gao and Pan, 2001; Tapon et al., 2001). A possible reason for this difference is that the mutant larval disc cells continue to divide, thereby maintaining a moderate cell size. One key question that remains is why the larval disc cells that contain a *TSC* mutation have somewhat coordinated growth and division, whereas the adult mutant ISCs have completely stopped their division. It is possible that because imaginal discs are developing organs, they are designed to have faster growth and division. Adult midgut ISCs have a slower intrinsic cell cycle of >24 h (Micchelli and Perrimon, 2006; Ohlstein and Spradling, 2006), and adult cells have differences in checkpoint controls (Su et al., 2000; Walworth, 2000; Song, 2005). These may allow the excessive growth to take place until it passes a critical point that blocks division.

Phenotypes manifested in TSC patients are mostly benign tumors that rarely progress into higher-grade cancers (Crino, 2008). TSC1 and 2 have expression in the intestine, and adult patients have occasional intestinal polyps (Hizawa et al., 1994; Fukuda et al., 2000; Johnson et al., 2001). Mouse embryonic fibroblasts from mutant *TSC* animals can also enter senescence, which is equivalent to a cessation of cell division (Zhang et al., 2007). The adult midgut ISC phenotypes shown in this study are consistent with these phenotypes. We speculate that excessive cell growth leading to a block in cell division is a common phenotype in slowly dividing adult tissues when *TSC* is mutated. The phenotype of increased cell growth and increased cell division may be applicable to rapidly dividing cells, including developing *Drosophila* disc cells, mammalian hematopoietic stem cells, and tumor cells (Ito and Rubin, 1999; Gao and Pan, 2001; Tapon et al., 2001; Rosner et al., 2006; Gan et al., 2008). A recent study demonstrates that in *TSC* mutants, there is loss of adult female germline stem cells because of differentiation (Sun et al., 2010). The ISCs and germline stem cells have different niche compositions that may contribute to the observed differences in the mutant phenotype. Moreover, it underscores the idea of a tissue context–dependent phenotype exhibited in *TSC* mutants.

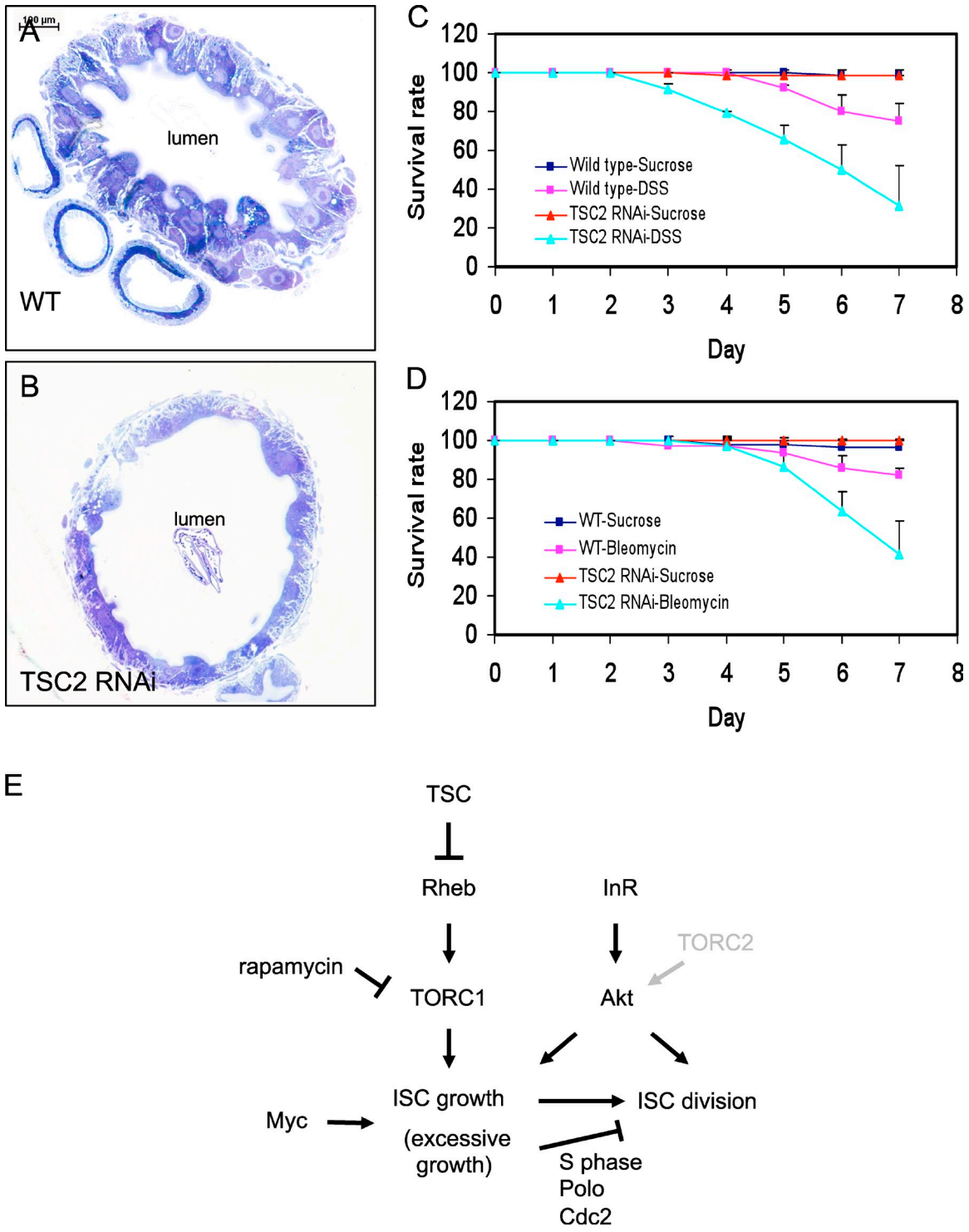

Figure 8. **Loss of TSC leads to impaired intestinal homeostasis.** (A and B) Midgut morphology in wild-type (WT) and *TSC2* RNAi flies. The dissected guts were mounted in Epon plastic, and after sectioning, the tissues were stained with Toluidine blue. In the wild-type gut, the enterocytes are more tightly packed around the lumen, and protrusions are seen in most enterocytes. In the *TSC2* RNAi gut, the enterocytes still form a continuous epithelium, but there are fewer protrusions, and there are fewer enterocytes in each section. The overall gut appeared thinner and smoother. (C and D) Wild type were esg>GFP;tubulin Gal80^{ts} flies. Feeding experiments were performed at 29°C. Wild-type and *TSC2* RNAi flies were fed with 5% sucrose as a control or with added 1% DSS or 2 μg/ml bleomycin. Flies were counted and transferred to new feeding vials every day. The survival rate is shown as a percentage. *TSC2* RNAi flies have increased susceptibility toward the two tissue-damaging agents. Three independent experiments were performed with 100 flies for each sample. (E) A model for TSC coordination of ISC growth and division through the TORC1 pathway. Both TORC1 and InR pathways can stimulate growth and division but appear to act independently in adult midgut ISCs. TSC inhibits TORC1 and ISC growth. In the absence of TSC, TORC1 stimulates an excessive growth, which leads to the inhibition of ISC division. The TORC2 function is dispensable in ISC growth and division. Myc may act independently to regulate ISC growth, but reducing Myc is sufficient to suppress the excessive growth induced by loss of TSC. The arrows indicate activation, and the lines with a bar end indicates repression. Error bars are standard deviations.

Materials and methods

Drosophila stocks and feeding experiments

Most stocks have been previously described in Amcheslavsky et al. (2009). *Myc* RNAi lines were obtained from VDRC, and the Transgenic RNAi Project, UAS-Myc, and *PTEN* RNAi lines were obtained from the Bloomington stock center (no. 8549). Polo-GFP (no. CC01326) was obtained from FlyTrap, and the *sin1* and *rictor* mutants were obtained from S. Cohen (Temasek Life Sciences Laboratory, Singapore; Hietakangas and Cohen, 2007), and the TOR flies were obtained from E. Baehrecke (University of Massachusetts, Worcester, MA) and T. Neufeld (University of Minnesota, Minneapolis, MN). Viability tests and feeding experiments were previously described in Amcheslavsky et al. (2009). In brief, 50–100 flies of 3–5 d old were used per vial. The vial contained a piece of 2.5 × 3.75–cm chromatography paper (Thermo Fisher Scientific). 500 µl of 5% sucrose solution was used to wet the paper as a feeding medium. The chemicals included in the feeding medium were 1% DSS (MP Biomedicals) or 2 µg/ml bleomycin (Sigma-Aldrich). Flies that were still alive were transferred to new vials with fresh feeding media every day. The MARCM clones were generated as previously described (Lee and Luo, 2001; Amcheslavsky et al., 2009). Flies stocks were crossed to generate the following genotype: *hsFLP,UAS-CD8GFP;esgGal4/+;FRT80B tubGal80/FRT80B TSC*^{192}. The final cross and offspring were maintained at 18°C. To induce MARCM clones, flies were heat shocked in a 37°C water bath for 30 min twice a day for 3 d. The flies were kept at 29°C and incubated for an additional 4–12 d before dissection.

For rapamycin feeding, 1 µl of 5.5-mM rapamycin (Sigma-Aldrich) dissolved in DMSO was added to 500 µl of a 20% sucrose solution. This mixture was added to standard fly food vials. The effective concentration in the food medium was ∼0.5 µM. 1-d-old flies were cultured on the rapamycin-augmented food, incubated at 29°C, and transferred to new media with rapamycin every 2 d over a period of 6–10 d. For EdU labeling, wild-type and *TSC2* mutant flies were fed on 100 µM EdU (Invitrogen) in a 5% sucrose solution for 24 h. Guts were dissected and subjected to Delta antibody staining as described previously (Amcheslavsky et al, 2009). EdU incorporation was detected using EdU Alexa Fluor 555 heat shock assay (Click-iT; Invitrogen) following the manufacturer's instructions.

Immunostaining and fluorescent microscopy

Most gut dissection, fixation, antibody staining, and confocal microscopy procedures were previously described in Amcheslavsky et al. (2009). The entire gastrointestinal tract was pulled from the posterior end directly into fixation medium containing PBS and 4% formaldehyde (Mallinckrodt Chemicals). Guts were fixed in this medium for 3 h, except for Delta staining in which the fixation was for 0.5 h. Subsequent rinses, washes, and incubations with primary and secondary antibodies were performed in a solution containing PBS, 0.5% BSA, and 0.1% Triton X-100. Anti-Cdc2 (rabbit polyclonal, 1:500 dilution; Santa Cruz Biotechnology, Inc.; a gift from W. Theurkauf, University of Massachusetts, Worcester, MA), anti-Pdm1 (rabbit polyclonal, 1:100 dilution; a gift from X. Yang, University of Singapore, Singapore), anti-AcH3 (rabbit polyclonal, 1:500 dilution; Millipore), and anti-GFP (rabbit polyclonal, 1:1,000 dilution; Invitrogen) were used for immunofluorescent staining. For Western blotting, the anti–C-terminal phospho-AKT antibody (rabbit polyclonal, 1:1,000 dilution; Cell Signaling Technology) and the antitubulin antibody (1:100 dilution; Hybridoma bank) were used.

Microscope image acquisition was performed in the Digital Light Microscopy Core Facility at the University of Massachusetts Medical School using a spinning-disk confocal microscope (Nikon). The main components are an inverted microscope (TE-2000E2; Nikon) with a spinning-disk confocal attachment (CSU10; Yokogawa) and a 40× Plan Apochromat oil objective (Nikon) with a numerical aperture of 1.0. The imaging temperature was room temperature, and the medium was oil. The fluorochromes used were DAPI, Alexa 488, Alexa 568, and Alexa 633. The camera make was a Rolera MGi EM charge-coupled device (QImaging). The acquisition and processing software was MetaMorph (Molecular Devices) with no deconvolution or γ adjustment and used an 8-bit export file format.

Gut dissection, tissue section, tissue dissociation, cell sorting, and RT-PCR

Guts dissection and sectioning were previously described in Amcheslavsky et al. (2009). For tissue dissociation, the malpighian tubules, the esophagus, and the rectum were removed, leaving only the midgut. Approximately 30 midguts were put into a 1.5-ml microfuge tube on ice containing a 0.5-ml solution of PBS, 1 mM EDTA, and 0.5% trypsin (Invitrogen). The tissues were incubated at room temperature for 2.5 h in the trypsin solution on a Nutator (Adams; BD) and vortexed vigorously every 30 min during the incubation. At the end of the incubation, the tissues were disrupted by a hand-held homogenizer. The dissociation of cells was confirmed by examining a small fraction of the suspension under a fluorescent microscope (TE-2000E2). DNA dye Hoechst 33342 (Roche) was added to the trypsin solution during cell dissociation at a final concentration of 10 µg/ml. The samples were stored on ice in the dark until analyzed. The cell suspensions were filtered through nylon mesh to remove large debris before passing through the cell sorter (LSR II; BD). S2 cells were used for preruns of the cell sorter. These cells were washed once with PBS, resuspended in PBS, 5 mM EDTA, and 10 µg/ml Hoechst 33342, and incubated for 2.5 h at room temperature. The cells were analyzed by a cell analyzer (LSR; BD; Flow Cytometry Core Facility, University of Massachusetts Medical School).

For real-time quantitative PCR, total RNA was isolated from 10 dissected guts and used to prepare cDNA. PCR was performed using a real-time PCR detection system (iQ5; Bio-Rad Laboratories) with the following primers: *TSC2* forward, 5′-ATCGTTGAGCCACTTGACCT-3′; *TSC2* reverse, 5′-TGCGTGGCACAGGAATTT-3′; *TSC1* forward, 5′-GCAAGGAGCAAAGAATCG-3′; *TSC1* reverse, 5′-ACTCATTGGCCTTGATCG-3′; *extra* (CG6634) forward, 5′-ACATTCAGCACCACAGCA-3′; *extra* reverse, 5′-TGATTGCTGCCCTGATCGTA-3′; *actin* forward, 5′-AGTGTGTGCAGCGGATAACT-3′; *actin* reverse, 5′-AAGCTGCAACCTCTTCGTCA-3′; *rp49* forward, 5′-CGGATGGATATGCTAAGCTGT-3′; and *rp49* reverse, 5′-GCGCTTGTTCGATCCGTA-3′. *rp49* was used as a normalization standard. RT–quantitative PCR was performed in duplicate on each of three independent biological replicates.

We thank M. Chatterjee, N. Mohammad, and N. Wakabayashi-Ito for help with cell dissociation experiments and David Guertin for comments on the manuscript. We thank S. Cohen for the *rictor* mutant flies, FlyTrap for the Polo-GFP line originated from the A. Spradling laboratory, E. Baehrecke and T. Neufeld for TOR transgenic lines, W. Theurkauf for the Cdc2 antibody, and X. Yang for the Pdm1 antibody.

The work in the Y.T. Ip laboratory was supported by grants from the National Institutes of Health (DK83450) and the Worcester Foundation for Biomedical Research. Y.T. Ip is a member of the University of Massachusetts Diabetes Endocrinology Research Center, and core resources supported by the center grant (DK32520) were also used. The work in the J. Jiang laboratory was supported by grants from the National Institutes of Health (GM61269 and GM67045), the Welch Foundation (I-1603), and the Cancer Prevention Research Institute of Texas (RP100561).

Submitted: 2 March 2011
Accepted: 18 April 2011

References

Amcheslavsky, A., J. Jiang, and Y.T. Ip. 2009. Tissue damage-induced intestinal stem cell division in *Drosophila*. *Cell Stem Cell*. 4:49–61. doi:10.1016/j.stem.2008.10.016

Apidianakis, Y., C. Pitsouli, N. Perrimon, and L. Rahme. 2009. Synergy between bacterial infection and genetic predisposition in intestinal dysplasia. *Proc. Natl. Acad. Sci. USA*. 106:20883–20888. doi:10.1073/pnas.0911797106

Avruch, J., K. Hara, Y. Lin, M. Liu, X. Long, S. Ortiz-Vega, and K. Yonezawa. 2006. Insulin and amino-acid regulation of mTOR signaling and kinase activity through the Rheb GTPase. *Oncogene*. 25:6361–6372. doi:10.1038/sj.onc.1209882

Bardin, A.J., C.N. Perdigoto, T.D. Southall, A.H. Brand, and F. Schweisguth. 2010. Transcriptional control of stem cell maintenance in the *Drosophila* intestine. *Development*. 137:705–714. doi:10.1242/dev.039404

Barker, N., J.H. van Es, J. Kuipers, P. Kujala, M. van den Born, M. Cozijnsen, A. Haegebarth, J. Korving, H. Begthel, P.J. Peters, and H. Clevers. 2007. Identification of stem cells in small intestine and colon by marker gene Lgr5. *Nature*. 449:1003–1007. doi:10.1038/nature06196

Barker, N., M. van de Wetering, and H. Clevers. 2008. The intestinal stem cell. *Genes Dev.* 22:1856–1864. doi:10.1101/gad.1674008

Barker, N., R.A. Ridgway, J.H. van Es, M. van de Wetering, H. Begthel, M. van den Born, E. Danenberg, A.R. Clarke, O.J. Sansom, and H. Clevers. 2009. Crypt stem cells as the cells-of-origin of intestinal cancer. *Nature*. 457:608–611. doi:10.1038/nature07602

Batlle, E. 2008. A new identity for the elusive intestinal stem cell. *Nat. Genet.* 40:818–819. doi:10.1038/ng0708-818

Beebe, K., W.C. Lee, and C.A. Micchelli. 2010. JAK/STAT signaling coordinates stem cell proliferation and multilineage differentiation in the *Drosophila* intestinal stem cell lineage. *Dev. Biol.* 338:28–37. doi:10.1016/j.ydbio.2009.10.045

Biteau, B., and H. Jasper. 2011. EGF signaling regulates the proliferation of intestinal stem cells in *Drosophila*. *Development*. 138:1045–1055. doi:10.1242/dev.056671

Biteau, B., C.E. Hochmuth, and H. Jasper. 2008. JNK activity in somatic stem cells causes loss of tissue homeostasis in the aging *Drosophila* gut. *Cell Stem Cell*. 3:442–455. doi:10.1016/j.stem.2008.07.024

Boheler, K.R. 2009. Stem cell pluripotency: a cellular trait that depends on transcription factors, chromatin state and a checkpoint deficient cell cycle. *J. Cell. Physiol.* 221:10–17. doi:10.1002/jcp.21866

Bray, S.J. 2006. Notch signalling: a simple pathway becomes complex. *Nat. Rev. Mol. Cell Biol.* 7:678–689. doi:10.1038/nrm2009

Buchon, N., N.A. Broderick, S. Chakrabarti, and B. Lemaitre. 2009a. Invasive and indigenous microbiota impact intestinal stem cell activity through multiple pathways in *Drosophila*. *Genes Dev.* 23:2333–2344. doi:10.1101/gad.1827009

Buchon, N., N.A. Broderick, M. Poidevin, S. Pradervand, and B. Lemaitre. 2009b. *Drosophila* intestinal response to bacterial infection: activation of host defense and stem cell proliferation. *Cell Host Microbe*. 5:200–211. doi:10.1016/j.chom.2009.01.003

Buchon, N., N.A. Broderick, T. Kuraishi, and B. Lemaitre. 2010. *Drosophila* EGFR pathway coordinates stem cell proliferation and gut remodeling following infection. *BMC Biol.* 8:152. doi:10.1186/1741-7007-8-152

Buszczak, M., S. Paterno, and A.C. Spradling. 2009. *Drosophila* stem cells share a common requirement for the histone H2B ubiquitin protease scrawny. *Science*. 323:248–251. doi:10.1126/science.1165678

Casali, A., and E. Batlle. 2009. Intestinal stem cells in mammals and *Drosophila*. *Cell Stem Cell*. 4:124–127. doi:10.1016/j.stem.2009.01.009

Chatterjee, M., and Y.T. Ip. 2009. Pathogenic stimulation of intestinal stem cell response in *Drosophila*. *J. Cell. Physiol.* 220:664–671. doi:10.1002/jcp.21808

Choi, N.H., J.G. Kim, D.J. Yang, Y.S. Kim, and M.A. Yoo. 2008. Age-related changes in *Drosophila* midgut are associated with PVF2, a PDGF/VEGF-like growth factor. *Aging Cell*. 7:318–334. doi:10.1111/j.1474-9726.2008.00380.x

Crino, P.B. 2008. Do we have a cure for tuberous sclerosis complex? *Epilepsy Curr.* 8:159–162. doi:10.1111/j.1535-7511.2008.00279.x

Cronin, S.J., N.T. Nehme, S. Limmer, S. Liegeois, J.A. Pospisilik, D. Schramek, A. Leibbrandt, Rde.M. Simoes, S. Gruber, U. Puc, et al. 2009. Genome-wide RNAi screen identifies genes involved in intestinal pathogenic bacterial infection. *Science*. 325:340–343. doi:10.1126/science.1173164

Crosnier, C., D. Stamataki, and J. Lewis. 2006. Organizing cell renewal in the intestine: stem cells, signals and combinatorial control. *Nat. Rev. Genet.* 7:349–359. doi:10.1038/nrg1840

Fukuda, T., T. Kobayashi, S. Momose, H. Yasui, and O. Hino. 2000. Distribution of Tsc1 protein detected by immunohistochemistry in various normal rat tissues and the renal carcinomas of Eker rat: detection of limited colocalization with Tsc1 and Tsc2 gene products in vivo. *Lab. Invest.* 80:1347–1359.

Gan, B., E. Sahin, S. Jiang, A. Sanchez-Aguilera, K.L. Scott, L. Chin, D.A. Williams, D.J. Kwiatkowski, and R.A. DePinho. 2008. mTORC1-dependent and -independent regulation of stem cell renewal, differentiation, and mobilization. *Proc. Natl. Acad. Sci. USA*. 105:19384–19389. doi:10.1073/pnas.0810584105

Gao, X., and D. Pan. 2001. TSC1 and TSC2 tumor suppressors antagonize insulin signaling in cell growth. *Genes Dev.* 15:1383–1392. doi:10.1101/gad.901101

Grewal, S.S., and B.A. Edgar. 2003. Controlling cell division in yeast and animals: does size matter? *J. Biol.* 2:5. doi:10.1186/1475-4924-2-5

Guertin, D.A., D.M. Stevens, C.C. Thoreen, A.A. Burds, N.Y. Kalaany, J. Moffat, M. Brown, K.J. Fitzgerald, and D.M. Sabatini. 2006. Ablation in mice of the mTORC components raptor, rictor, or mLST8 reveals that mTORC2 is required for signaling to Akt-FOXO and PKCalpha, but not S6K1. *Dev. Cell*. 11:859–871. doi:10.1016/j.devcel.2006.10.007

Guertin, D.A., D.M. Stevens, M. Saitoh, S. Kinkel, K. Crosby, J.H. Sheen, D.J. Mullholland, M.A. Magnuson, H. Wu, and D.M. Sabatini. 2009. mTOR complex 2 is required for the development of prostate cancer induced by Pten loss in mice. *Cancer Cell*. 15:148–159. doi:10.1016/j.ccr.2008.12.017

Hietakangas, V., and S.M. Cohen. 2007. Re-evaluating AKT regulation: role of TOR complex 2 in tissue growth. *Genes Dev.* 21:632–637. doi:10.1101/gad.416307

Hizawa, K., M. Iida, T. Matsumoto, M. Tominaga, C. Hirota, T. Yao, and M. Fujishima. 1994. Gastrointestinal involvement in tuberous sclerosis. Two case reports. *J. Clin. Gastroenterol.* 19:46–49. doi:10.1097/00004836-199407000-00012

Hsu, H.J., and D. Drummond-Barbosa. 2009. Insulin levels control female germline stem cell maintenance via the niche in *Drosophila*. *Proc. Natl. Acad. Sci. USA*. 106:1117–1121. doi:10.1073/pnas.0809144106

Huang, J., and B.D. Manning. 2008. The TSC1-TSC2 complex: a molecular switchboard controlling cell growth. *Biochem. J.* 412:179–190. doi:10.1042/BJ20080281

Huang, J., and B.D. Manning. 2009. A complex interplay between Akt, TSC2 and the two mTOR complexes. *Biochem. Soc. Trans.* 37:217–222. doi:10.1042/BST0370217

Huang, J., S. Wu, C.L. Wu, and B.D. Manning. 2009. Signaling events downstream of mammalian target of rapamycin complex 2 are attenuated in cells and tumors deficient for the tuberous sclerosis complex tumor suppressors. *Cancer Res.* 69:6107–6114. doi:10.1158/0008-5472.CAN-09-0975

Inoki, K., and K.L. Guan. 2009. Tuberous sclerosis complex, implication from a rare genetic disease to common cancer treatment. *Hum. Mol. Genet.* 18:R94–R100. doi:10.1093/hmg/ddp032

Ito, N., and G.M. Rubin. 1999. gigas, a *Drosophila* homolog of tuberous sclerosis gene product-2, regulates the cell cycle. *Cell*. 96:529–539. doi:10.1016/S0092-8674(00)80657-1

Jiang, H., and B.A. Edgar. 2009. EGFR signaling regulates the proliferation of *Drosophila* adult midgut progenitors. *Development*. 136:483–493. doi:10.1242/dev.026955

Jiang, H., P.H. Patel, A. Kohlmaier, M.O. Grenley, D.G. McEwen, and B.A. Edgar. 2009. Cytokine/Jak/Stat signaling mediates regeneration and homeostasis in the *Drosophila* midgut. *Cell*. 137:1343–1355. doi:10.1016/j.cell.2009.05.014

Jiang, H., M.O. Grenley, M.J. Bravo, R.Z. Blumhagen, and B.A. Edgar. 2011. EGFR/Ras/MAPK signaling mediates adult midgut epithelial homeostasis and regeneration in *Drosophila*. *Cell Stem Cell*. 8:84–95. doi:10.1016/j.stem.2010.11.026

Johnson, M.W., C. Kerfoot, T. Bushnell, M. Li, and H.V. Vinters. 2001. Hamartin and tuberin expression in human tissues. *Mod. Pathol.* 14:202–210. doi:10.1038/modpathol.3880286

Johnston, L.A., D.A. Prober, B.A. Edgar, R.N. Eisenman, and P. Gallant. 1999. *Drosophila* myc regulates cellular growth during development. *Cell*. 98:779–790. doi:10.1016/S0092-8674(00)81512-3

Jorgensen, P., and M. Tyers. 2004. How cells coordinate growth and division. *Curr. Biol.* 14:R1014–R1027. doi:10.1016/j.cub.2004.11.027

Karpowicz, P., J. Perez, and N. Perrimon. 2010. The Hippo tumor suppressor pathway regulates intestinal stem cell regeneration. *Development*. 137:4135–4145. doi:10.1242/dev.060483

Kohlmaier, A., and B.A. Edgar. 2008. Proliferative control in *Drosophila* stem cells. *Curr. Opin. Cell Biol.* 20:699–706. doi:10.1016/j.ceb.2008.10.002

Lee, T., and L. Luo. 2001. Mosaic analysis with a repressible cell marker (MARCM) for *Drosophila* neural development. *Trends Neurosci.* 24:251–254. doi:10.1016/S0166-2236(00)01791-4

Lee, W.C., K. Beebe, L. Sudmeier, and C.A. Micchelli. 2009. Adenomatous polyposis coli regulates *Drosophila* intestinal stem cell proliferation. *Development*. 136:2255–2264. doi:10.1242/dev.035196

Leevers, S.J., and H. McNeill. 2005. Controlling the size of organs and organisms. *Curr. Opin. Cell Biol.* 17:604–609. doi:10.1016/j.ceb.2005.09.008

Li, L., and H. Clevers. 2010. Coexistence of quiescent and active adult stem cells in mammals. *Science*. 327:542–545. doi:10.1126/science.1180794

Lin, G., N. Xu, and R. Xi. 2008. Paracrine Wingless signalling controls self-renewal of *Drosophila* intestinal stem cells. *Nature*. 455:1119–1123. doi:10.1038/nature07329

Lin, G., N. Xu, and R. Xi. 2010. Paracrine unpaired signaling through the JAK/STAT pathway controls self-renewal and lineage differentiation of *Drosophila* intestinal stem cells. *J. Mol. Cell Biol.* 2:37–49. doi:10.1093/jmcb/mjp028

Llamazares, S., A. Moreira, A. Tavares, C. Girdham, B.A. Spruce, C. Gonzalez, R.E. Karess, D.M. Glover, and C.E. Sunkel. 1991. polo encodes a protein kinase homolog required for mitosis in *Drosophila*. *Genes Dev.* 5:2153–2165. doi:10.1101/gad.5.12a.2153

Maeda, K., M. Takemura, M. Umemori, and T. Adachi-Yamada. 2008. E-cadherin prolongs the moment for interaction between intestinal stem cell and its progenitor cell to ensure Notch signaling in adult *Drosophila* midgut. *Genes Cells*. 13:1219–1227. doi:10.1111/j.1365-2443.2008.01239.x

Mathur, D., A. Bost, I. Driver, and B. Ohlstein. 2010. A transient niche regulates the specification of *Drosophila* intestinal stem cells. *Science*. 327:210–213. doi:10.1126/science.1181958

Metcalfe, A.D., and M.W. Ferguson. 2008. Skin stem and progenitor cells: using regeneration as a tissue-engineering strategy. *Cell. Mol. Life Sci.* 65:24–32. doi:10.1007/s00018-007-7427-x

Micchelli, C.A., and N. Perrimon. 2006. Evidence that stem cells reside in the adult *Drosophila* midgut epithelium. *Nature*. 439:475–479. doi:10.1038/nature04371

Montgomery, R.K., and D.T. Breault. 2008. Small intestinal stem cell markers. *J. Anat.* 213:52–58. doi:10.1111/j.1469-7580.2008.00925.x

Niemeyer, P., U. Krause, P. Kasten, P.C. Kreuz, P. Henle, N.P. Südkam, and A. Mehlhorn. 2006. Mesenchymal stem cell-based HLA-independent cell therapy for tissue engineering of bone and cartilage. *Curr. Stem Cell Res. Ther.* 1:21–27. doi:10.2174/157488806775269151

Nystul, T.G., and A.C. Spradling. 2006. Breaking out of the mold: diversity within adult stem cells and their niches. *Curr. Opin. Genet. Dev.* 16:463–468. doi:10.1016/j.gde.2006.08.003

Ohlstein, B., and A. Spradling. 2006. The adult *Drosophila* posterior midgut is maintained by pluripotent stem cells. *Nature*. 439:470–474. doi:10.1038/nature04333

Ohlstein, B., and A. Spradling. 2007. Multipotent *Drosophila* intestinal stem cells specify daughter cell fates by differential notch signaling. *Science*. 315:988–992. doi:10.1126/science.1136606

Pan, D., J. Dong, Y. Zhang, and X. Gao. 2004. Tuberous sclerosis complex: from *Drosophila* to human disease. *Trends Cell Biol.* 14:78–85. doi:10.1016/j.tcb.2003.12.006

Park, J.S., Y.S. Kim, and M.A. Yoo. 2009. The role of p38b MAPK in age-related modulation of intestinal stem cell proliferation and differentiation in *Drosophila*. *Aging (Albany NY)*. 1:637–651.

Ren, F., B. Wang, T. Yue, E.Y. Yun, Y.T. Ip, and J. Jiang. 2010. Hippo signaling regulates *Drosophila* intestine stem cell proliferation through multiple pathways. *Proc. Natl. Acad. Sci. USA*. 107:21064–21069. doi:10.1073/pnas.1012759107

Rosner, M., A. Freilinger, and M. Hengstschläger. 2006. The tuberous sclerosis genes and regulation of the cyclin-dependent kinase inhibitor p27. *Mutat. Res.* 613:10–16. doi:10.1016/j.mrrev.2006.03.001

Royou, A., D. McCusker, D.R. Kellogg, and W. Sullivan. 2008. Grapes(Chk1) prevents nuclear CDK1 activation by delaying cyclin B nuclear accumulation. *J. Cell Biol.* 183:63–75. doi:10.1083/jcb.200801153

Sang, Y., M.F. Wu, and D. Wagner. 2009. The stem cell—chromatin connection. *Semin. Cell Dev. Biol.* 20:1143–1148. doi:10.1016/j.semcdb.2009.09.006

Sangiorgi, E., and M.R. Capecchi. 2008. Bmi1 is expressed in vivo in intestinal stem cells. *Nat. Genet.* 40:915–920. doi:10.1038/ng.165

Sarbassov, D.D., D.A. Guertin, S.M. Ali, and D.M. Sabatini. 2005. Phosphorylation and regulation of Akt/PKB by the rictor-mTOR complex. *Science*. 307:1098–1101. doi:10.1126/science.1106148

Schmidt, E.V., M.J. Ravitz, L. Chen, and M. Lynch. 2009. Growth controls connect: interactions between c-myc and the tuberous sclerosis complex-mTOR pathway. *Cell Cycle*. 8:1344–1351. doi:10.4161/cc.8.9.8215

Scoville, D.H., T. Sato, X.C. He, and L. Li. 2008. Current view: intestinal stem cells and signaling. *Gastroenterology*. 134:849–864. doi:10.1053/j.gastro.2008.01.079

Shaw, R.L., A. Kohlmaier, C. Polesello, C. Veelken, B.A. Edgar, and N. Tapon. 2010. The Hippo pathway regulates intestinal stem cell proliferation during *Drosophila* adult midgut regeneration. *Development*. 137:4147–4158. doi:10.1242/dev.052506

Song, Y.H. 2005. *Drosophila melanogaster*: a model for the study of DNA damage checkpoint response. *Mol. Cells*. 19:167–179.

Staley, B.K., and K.D. Irvine. 2010. Warts and Yorkie mediate intestinal regeneration by influencing stem cell proliferation. *Curr. Biol.* 20:1580–1587. doi:10.1016/j.cub.2010.07.041

Su, T.T., J. Walker, and J. Stumpff. 2000. Activating the DNA damage checkpoint in a developmental context. *Curr. Biol.* 10:119–126. doi:10.1016/S0960-9822(00)00300-6

Sun, P., Z. Quan, B. Zhang, T. Wu, and R. Xi. 2010. TSC1/2 tumour suppressor complex maintains *Drosophila* germline stem cells by preventing differentiation. *Development*. 137:2461–2469. doi:10.1242/dev.051466

Tapon, N., N. Ito, B.J. Dickson, J.E. Treisman, and I.K. Hariharan. 2001. The *Drosophila* tuberous sclerosis complex gene homologs restrict cell growth and cell proliferation. *Cell*. 105:345–355. doi:10.1016/S0092-8674(01)00332-4

Teleman, A.A., V. Hietakangas, A.C. Sayadian, and S.M. Cohen. 2008. Nutritional control of protein biosynthetic capacity by insulin via Myc in *Drosophila*. *Cell Metab.* 7:21–32. doi:10.1016/j.cmet.2007.11.010

Walker, M.R., and T.S. Stappenbeck. 2008. Deciphering the 'black box' of the intestinal stem cell niche: taking direction from other systems. *Curr. Opin. Gastroenterol.* 24:115–120. doi:10.1097/MOG.0b013e3282f4954f

Walworth, N.C. 2000. Cell-cycle checkpoint kinases: checking in on the cell cycle. *Curr. Opin. Cell Biol.* 12:697–704. doi:10.1016/S0955-0674(00)00154-X

Wu, D.C., and L.A. Johnston. 2010. Control of wing size and proportions by *Drosophila* myc. *Genetics*. 184:199–211. doi:10.1534/genetics.109.110379

Yen, T.H., and N.A. Wright. 2006. The gastrointestinal tract stem cell niche. *Stem Cell Rev.* 2:203–212. doi:10.1007/s12015-006-0048-1

Zhang, H., N. Bajraszewski, E. Wu, H. Wang, A.P. Moseman, S.L. Dabora, J.D. Griffin, and D.J. Kwiatkowski. 2007. PDGFRs are critical for PI3K/Akt activation and negatively regulated by mTOR. *J. Clin. Invest.* 117:730–738. doi:10.1172/JCI28984

Zhu, L., P. Gibson, D.S. Currle, Y. Tong, R.J. Richardson, I.T. Bayazitov, H. Poppleton, S. Zakharenko, D.W. Ellison, and R.J. Gilbertson. 2009. Prominin 1 marks intestinal stem cells that are susceptible to neoplastic transformation. *Nature*. 457:603–607. doi:10.1038/nature07589